



**Temperature responsive hydrogel with ultra large solar modulation and high luminous transmission for smart window applications**

Journal:	<i>Journal of Materials Chemistry A</i>
Manuscript ID:	TA-ART-05-2014-002287.R1
Article Type:	Paper
Date Submitted by the Author:	03-Jun-2014
Complete List of Authors:	Zhou, Yang; Nanyang Technological University, School of materials science and engineering Cai, Yufeng; Nanyang Technological University, School of materials science and engineering Hu, Xiao; Nanyang Technological University, School of Materials Sci & Eng Long, Yi; Nanyang Technological University,

## Temperature responsive hydrogel with ultra large solar modulation and high luminous transmission for smart window applications

Yang Zhou<sup>†</sup>, Yufeng Cai<sup>†</sup>, Xiao Hu<sup>\*</sup>, Yi Long<sup>\*</sup>

School of Materials Science and Engineering, Nanyang Technological University, 50

Nanyang Avenue, Singapore, 639798

\*Corresponding authors

Dr Yi Long, E-mail: longyi@ntu.edu.sg

Professor Xiao Hu, Tel.: (65)6790 4610, (65) 6790 9081, E-mail: asxhu@ntu.edu.sg.

<sup>†</sup> Authors contributed equally

### Abstract

The application of PNIPAm hydrogel thin film for thermochromic smart windows has been investigated for the first time. With increasing thickness of hydrogel from 26 to 200  $\mu\text{m}$  and increasing testing temperature from 20  $^{\circ}\text{C}$  to 60  $^{\circ}\text{C}$ , the solar modulating ability ( $\Delta T_{\text{sol}}$ ) increases and the luminous transmittance ( $T_{\text{lum}}$ ) decreases. Compared with the best reported result of the most studied inorganic  $\text{VO}_2$  thermochromic coatings, an unprecedented good combination of near doubled averaged  $T_{\text{lum}}$  (70.7% v.s 42.8%), higher  $\Delta T_{\text{sol}}$  (25.5% v.s 22.3%) and lower transition temperature ( $\sim 32$   $^{\circ}\text{C}$  v.s  $\sim 68$   $^{\circ}\text{C}$ ) could be achieved by hydrogel with optimized thickness. Good durability and reversibility were established on proper sealing of the sandwich structure, thereby achieving a new milestone in the research for organic thermochromic materials.

**Key words:** Hydrogel, smart window, solar modulation, thermochromism

## Introduction

Smart window refers to the window which can control light transmission properties under the application of voltage (electrochromism),<sup>1</sup> light (photochromism)<sup>2</sup> or heat (thermochromism). Thermochromic material can be used as a passive and zero-energy input smart window, which can regulate the solar transmission by temperature stimulus for energy consumption reduction.<sup>3-5</sup> For example, when the outdoor temperature is higher than the critical point of the smart window, the transmission of solar light (250 nm~2500 nm) could be reduced to minimize the solar energy input and therefore, reduce indoor temperature to cut the electric energy consumption for air-conditioning. On the other hand, if the outdoor temperature declines below the critical point of smart window, the solar transmission could be increased to ensure maximum solar energy input. For ideal smart-windows, a large disparity in solar transmission at temperatures above and below critical temperature ( $\tau_c$ ) is desirable for a good solar energy modulation ( $\Delta T_{sol}$ ). Meanwhile the visible light (380 nm-780 nm) transmission ( $T_{lum}$ ) ideally should remain high (preferably larger than 70%)<sup>6</sup> to ensure good indoor luminous condition. In addition,  $\tau_c$  of such desirable smart window should be within the range of 25 °C to 35 °C.

Vanadium dioxide (VO<sub>2</sub>) based inorganic materials are the most widely studied candidates of smart windows<sup>7-9</sup> although they are haunted with problems of high transition temperature ( $\tau_c \sim 68^\circ\text{C}$ ) and low  $T_{lum}$  as well as low  $\Delta T_{sol}$ . Efforts to increase both  $T_{lum}$  and  $\Delta T_{sol}$  simultaneously include doping certain ions (such as Mg<sup>2+</sup>, Eu<sup>3+</sup> and Ti) into VO<sub>2</sub> crystal lattice,<sup>10-12</sup> depositing anti-reflection (AR) coatings,<sup>13-15</sup> tuning

porosity,<sup>16,17</sup> and integrating VO<sub>2</sub> nanoparticles with transparent matrix.<sup>18-20</sup> Meanwhile, the tactics in reducing transition temperature, e.g., introducing dopants (W<sup>6+</sup>, F<sup>-</sup> etc), would always inevitably sacrifice both  $T_{lum}$  and  $\Delta T_{sol}$ .<sup>21-23</sup> Some best reported results for VO<sub>2</sub> based material are  $\Delta T_{sol}$ =12% with averaged  $T_{lum}$ =59.1%,<sup>18</sup> and  $\Delta T_{sol}$ =22.3% with averaged  $T_{lum}$ =42.8%<sup>19</sup>.

We hereby report temperature responsive hydrogels as the new candidates for smart windows application. The temperature responsive hydrogels, including poly (vinyl methyl ether),<sup>24</sup> poly (vinylcaprolactame),<sup>25</sup> hydroxypropylcellulose<sup>26</sup> and poly (N-isopropylacryamide),<sup>27-30</sup> etc, can undergo a hydrophilic-to-hydrophobic transition at lower critical solution temperature (LCST).<sup>31-34</sup> In this paper poly (N-isopropylacryamide) (PNIPAm) as the candidate was chosen since it is the most typical temperature responsive hydrogel and its LCST (~32 °C) lies between the range of 25-35 °C that the smart windows prefer. Although the transition mechanism of PNIPAm<sup>35</sup> has been widely studied and applied for tissue engineering,<sup>36,37</sup> drug delivery<sup>38-41</sup> and sensors,<sup>42</sup> however its concomitant optical transition at LCST has been ignored due to the complete opaque state above LCST which is not desirable in the smart windows applications.<sup>43</sup> However by tuning the thickness of the hydrogel and designing suitable glass panel setup, the reversibly tunable transparency of PNIPAm hydrogels can be utilized in the smart windows application.

In this paper, we for the first time systematically studied the optical properties including  $\Delta T_{sol}$  and  $T_{lum}$  of the PNIPAm hydrogel with micrometers thicknesses below and above the transition temperature with hydrogel transiting from transparency to translucent above

LCST. This simple hydrogel demonstrates so far the highest  $T_{lum}$  (>70%, for saving lighting) together with the ultra large  $\Delta T_{sol}$  (for maximum solar modulation). Compared with traditional inorganic  $VO_2$ , the PNIPAm hydrogels are much easier to be manufactured and its LCST can be easily tuned<sup>44</sup> according to specific usage conditions of smart windows.

## Experimental

### Materials

Chemicals used in this study were N-isopropylacrylamine (NIPAAm,  $\geq 98\%$ , Wako Pure Chemical Industries Ltd), N, N'-methylenebis(acrylamide) ( $\geq 99\%$ , crosslinker, Sigma-Aldrich), polyvinyl alcohol (PVA,  $M_w = 61,000$ , Sigma-Aldrich) and N,N,N',N'-tetramethylethylenediamine (TEMED, accelerator, 99%, Sigma-Aldrich), ammonium peroxydisulfate (initiator, 98%, Alfa Aesar) and multipurpose sealant (Selley's All Clear). Deionized water (18.2 M $\Omega$ ) was used throughout the experiments. All were used as received without any further purification.

### Preparation of the sandwiched hydrogel structure

PNIPAm hydrogel was synthesized by in-situ polymerization of monomer in deionized (DI) water. In this case, 7.91 g (0.07 mol) N-Isopropylacrylamide (NIPAm), 1.32 g (0.03 mol) Polyvinyl alcohol (PVA), and 215.6 mg (0.0014 mol) N,N'-Methylenebis (acrylamide) were dissolved in 70 °C DI water to make a homogenous 100 ml aqueous solution. After the homogeneous and transparent solution was obtained, the temperature was reduced to 25 °C and this solution was purged with  $N_2$  for 30 minutes. 520.0  $\mu$ L of this stock solution was pipetted into one 1 mL centrifuge tube, and then 7.0  $\mu$ L

N,N,N',N''-Tetramethylethylenediamine (TEMED, catalyst) and 16.0  $\mu\text{L}$  ammonium persulfate (APS, initiator) were added in sequence to the centrifuge tube with vigorous vibration on vortex for 10 seconds. The solution was dropped on the surface of clean glass slide and covered by another one to make a sandwich structure after the reaction completed at room temperature for 24 hours. Samples with thickness of 26  $\mu\text{m}$ , 52  $\mu\text{m}$ , 78  $\mu\text{m}$  and 200  $\mu\text{m}$  were successfully made and the sealant was applied at the edges to prevent mass exchange with outside environment. Figure 1 shows the mechanism of laminated hydrogel thin film. When the hydrogel is below  $\tau_c$ , the transparency allows large transmission of solar radiation, while above  $\tau_c$  the phase separation induced scattering center partially blocks radiation, thereby reducing the transmission.<sup>45</sup>

### Characterization

The transmittance spectra in 250 nm – 2500 nm wavelength range were collected on a UV-Vis-NIR spectrophotometer (Cary 5000, Agilent, USA) at normal incidence. The spectrophotometer is equipped with a heating and cooling stage (PE120, Linkam, UK).

The integral luminous transmittance  $T_{\text{lum}}$  (380–780 nm), IR transmittance  $T_{\text{IR}}$  (780–2500 nm) and solar transmittance  $T_{\text{sol}}$  (250–2500 nm) were calculated by equation 1:

$$T_{\text{lum/IR/sol}} = \int \varphi_{\text{lum/IR/sol}}(\lambda)T(\lambda)d\lambda / \int \varphi_{\text{lum/IR/sol}}(\lambda)d\lambda \quad (1)$$

where  $T(\lambda)$  denotes spectral transmittance,  $\varphi_{\text{lum}}(\lambda)$  is the standard luminous efficiency function of photopic vision<sup>46</sup> in the wavelength range of 380–780 nm,  $\varphi_{\text{IR}}(\lambda)$  and  $\varphi_{\text{sol}}(\lambda)$

is the IR/solar irradiance spectrum for air mass 1.5 (corresponding to the sun standing 37° above the horizon).<sup>47</sup>  $\Delta T_{\text{lum/IR/sol}}$  is obtained by  $\Delta T_{\text{lum/IR/sol}} = T_{\text{lum/IR/sol}, 20\text{ }^\circ\text{C}} - T_{\text{lum/IR/sol}, 40\text{ }^\circ\text{C}}$ .

## Results and Discussion

Figure 2a and 2c shows the solar light transmittance (250 nm-2500 nm) profiles of PNIPAm hydrogels with thickness of 200  $\mu\text{m}$  and 52  $\mu\text{m}$  under various temperatures. According to Figure 2, two transmittance reductions happened at around 1430 nm and 1930 nm wavelength for both thick and thin samples, which is due to the absorption of water at these two wavelengths.<sup>48</sup> The absorption peak of water at around 1400nm is due to the O-H stretch in the water molecule, while at around 1900nm water has a unique peak due to a combination of O-H stretch and H-O-H bending.<sup>49</sup> At low temperature, more hydrogen bonds exist between water and PNIPAm polymer chains,<sup>50</sup> as temperature increases, these hydrogen bonds are gradually broken, which indicates a continuous phase separation. The oscillator strength of O-H bond is proportional to the hydrogen bond energy,<sup>51</sup> therefore, with fewer existing hydrogen bonds, the intensity of the transmittance valleys decreases.

For the thick PNIPAm hydrogel film with 200  $\mu\text{m}$  thickness, it maintained transparency below the LCST with the calculated  $T_{\text{lum}}$  of 89.1% at 20  $^\circ\text{C}$  and slightly reduced  $T_{\text{lum}}$  of 75% at 30  $^\circ\text{C}$  (Table 1). However, it turns into milky white at 35  $^\circ\text{C}$  with dramatically diminished  $T_{\text{lum}}$  of 7.3% and only 0.6% at 60  $^\circ\text{C}$  (Figure 2a, Table 1). The sharp decline of  $T_{\text{lum}}$  suggested that the LCST occurred at between 30  $^\circ\text{C}$  and 35  $^\circ\text{C}$ . The blocking effect around LCST was not only observed for luminance range but for infrared, which can be seen in Table 1 that the  $T_{\text{IR}}$  reduced from 79.4 to 48.4% significantly at 35  $^\circ\text{C}$

with further steady decline to 19.3% when the temperature reaches 60 °C. Both largely reduced  $T_{\text{IR}}$  and  $T_{\text{lum}}$  resulted in continuously declined  $T_{\text{sol}}$  from 83.3 to 9.4 % (Table 1), thereby leading to soared  $\Delta T_{\text{IR}}$ ,  $\Delta T_{\text{lum}}$  and  $\Delta T_{\text{sol}}$  between 30 and 40 °C and reached plateau afterwards with temperature increase (Figure 2b). Therefore, the effective blocking of both IR and visible light at temperature above LCST makes the overall solar modulating ability of PNIPAm hydrogel with 200  $\mu\text{m}$  thickness impressive ( $\sim 70\%$  at 40 °C), but the severely paralyzed luminance transmittance (1.2% at 40 °C) excludes the hydrogel with 200  $\mu\text{m}$  thickness from being applied in smart window.

In order to enhance the luminance transmittance at temperatures above LCST, the thickness of hydrogel was reduced to 52  $\mu\text{m}$  and the optical properties were shown in Figure 2c and 2d. The  $T_{\text{lum}}$  maintained at high level of higher than 50% even at 60 °C. Admittedly, the reduced thickness of hydrogels and consequently declined blocking abilities resulted in higher  $T_{\text{IR}}$ ,  $T_{\text{lum}}$  and  $T_{\text{sol}}$  (Table 2) at temperatures above LCST compared with 200  $\mu\text{m}$  hydrogel, however, the combined high luminance transmittance of  $>60\%$  and compromised solar modulating ability of  $>20\%$  (Figure 2d) at 40 °C are still higher than the best performing VO<sub>2</sub> thin films ( $T_{\text{lum}} \sim 54\%$  and  $\Delta T_{\text{sol}} \sim 12\%$  at 90 °C). Moreover,  $\Delta T_{\text{IR}}$ ,  $\Delta T_{\text{lum}}$  and  $\Delta T_{\text{sol}}$  increases progressively with temperature as shown in Figure 2d, which is preferable to ensure a relatively stable indoor temperature. Meanwhile, the transmittance is still higher than 50% even at 60 °C that a good indoor luminance is provided.

According to the discussion above, the potential of PNIPAm hydrogel thin film to be used in smart window application is related to the hydrogel's thickness. The thickness

effect of “thin” hydrogel was further studied within the thickness of less than 100  $\mu\text{m}$ . As can be seen from Figure 3a, the water absorption intensity at both 1930 nm and 1430 nm increased when the thickness increases from 26  $\mu\text{m}$  to 78  $\mu\text{m}$ , and the temperature decreased from 40  $^{\circ}\text{C}$  to 20  $^{\circ}\text{C}$  which is similar to Figure 2. As shown in Table 3, the  $T_{\text{lum}}(20^{\circ}\text{C})$  remained nearly unchanged for all 3 samples, while  $T_{\text{lum}}(40^{\circ}\text{C})$  underwent a monotonous reduction from  $\sim 80\%$  (26  $\mu\text{m}$ ) to less than 20% (78  $\mu\text{m}$ ). Although the hydrogel with 78  $\mu\text{m}$  thickness showed impressive  $\Delta T_{\text{sol}}$  of nearly 50%, its low  $T_{\text{lum}}(40^{\circ}\text{C})$  of less than 20% can be least satisfactory for ideal smart window. The compromise between  $T_{\text{lum}}$  at high temperature and  $\Delta T_{\text{sol}}$  also applied for hydrogel with thickness of 26  $\mu\text{m}$ . The extremely low thickness was accompanied by almost unchanged luminance transmittance as well as poor solar modulating ability at temperatures above LCST. The averaged  $T_{\text{lum}}(40^{\circ}\text{C})$  decreases with the thickness while  $\Delta T_{\text{lum}}$ ,  $\Delta T_{\text{IR}}$  and  $\Delta T_{\text{sol}}$  increases with thickness (Figure 3b).

The hydrogel with thickness of 52  $\mu\text{m}$  was picked to compare its thermochromic performance with one of the best reported  $\text{VO}_2$  samples to date.<sup>16</sup> As highlighted in Table 3, 52  $\mu\text{m}$  hydrogel sample has much higher  $T_{\text{lum}}$  at 20  $^{\circ}\text{C}$  (87.9% v.s 63.7%) and slightly higher  $T_{\text{lum}}$  at high temperature (59.9%<sub>(40  $^{\circ}\text{C}$ )</sub> v.s 54.4 %<sub>(90  $^{\circ}\text{C}$ )</sub>) which results in enhanced averaged  $T_{\text{lum}}$  (73.9% v.s 59.1%). In addition, hydrogel has much larger  $\Delta T_{\text{lum}}$  compared with  $\text{VO}_2$  (28.0% v.s. 9.3%) with reduced  $\Delta T_{\text{IR}}$  (9.5% v.s 17.2%). Since visible range has higher  $\varphi_{\text{sol}}(\lambda)$  compared with infrared range, the greatly enhanced  $\Delta T_{\text{lum}}$  resulted in nearly doubled solar modulating ability ( $\Delta T_{\text{sol}}$ , 20.4% v.s 12%) compared with  $\text{VO}_2$ , indicating a more effective modulation of solar radiation.

The actual outdoor test of hydrogels with various thicknesses was done in Singapore at atmospheric temperature of 35 °C in a sunny day. As shown in Figure 4, except the hydrogel with thickness of 26 μm that was proved with poor solar modulating, all other thicker hydrogels would become translucent or totally opaque within one minute outdoors and recover its transparency within one minute indoors. The outdoor translucency of hydrogels with thicknesses of 78 μm and 200 μm is too poor for windows, while the thickness of 52 μm shows acceptable outdoor transparency at high temperature.

Importantly, the good performance can be maintained in the durability test as shown in Figure 5, with consistent  $T_{lum}$  at both high and low temperature and relatively unchanged  $\Delta T_{sol}$  after 20 cycles of measurement, indicating that the performance stability should be reliable in actual smart window application as long as good sealing to prevent water evaporation is achieved. Considering the hydrogel's more suitable and easily tunable transition temperature, the temperature responsive hydrogels surpassed the best reported VO<sub>2</sub> films and should be one of the best candidates for thermochromic smart window application.

## Conclusion

Temperature responsive hydrogel delegated by the PNIPAm was investigated as potential novel alternative thermochromic material replacing traditional VO<sub>2</sub> for smart window application. With properly tuned thickness, hydrogel can be totally transparent at room temperature with high  $T_{lum}$  of 87.9% and translucent at 40 °C, with acceptable  $T_{lum}$  of 59.9%. Also, it can provide both high modulation in visible range and moderate

modulation ability in IR range, which lead to a largely overall enhanced  $\Delta T_{\text{sol}}$  (20-40 °C) of 20.4% or 25.5% for  $\Delta T_{\text{sol}}$  (20-60 °C) compared with the best reported VO<sub>2</sub> thermochromic film ( $\Delta T_{\text{sol}}$  (20-90 °C)  $\sim$  22.3%,  $T_{\text{lum}}$ (20°C) 45.6% and  $T_{\text{lum}}$ (90°C)  $\sim$  40.0%). This hydrogel demonstrated an unprecedented combination of high  $T_{\text{lum}}$ , dramatically improved  $\Delta T_{\text{sol}}$  and lowered transition temperature with good durability and reversibility, which is almost unlikely to be achieved by any modifications on current VO<sub>2</sub> based materials. The outperforming temperature responsive hydrogel would pave the road to the development of organic thermochromic smart windows.

### Acknowledgements

This research is supported by the Singapore National Research Foundation under CREATE programme: Nanomaterials for Energy and Water Management and Singapore minister of education (MOE) Academic Research Fund Tier 1 RG101/13. The electron microscopy and XRD work were performed at the Facility for Analysis, Characterization, Testing and Simulation (FACTS) in Nanyang Technological University, Singapore.

### References

1. K. Wang, H. Wu, Y. Meng, Y. Zhang and Z. Wei, *Energy Environ.Sci.*, 2012, **5**, 8384-8389
2. S. Papaefthimiou, *Advances in Building Energy Research*, 2010, **4:1**, 77-126.
3. M. Saeli, C. Piccirillo, I. P. Parkin, I. Ridley and R. Binions, *Sol. Energy Mater. Sol. Cells*, 2010, **94**, 141-151.
4. L. Kang, Y. Gao, Z. Zhang, J. Du, C. Cao, Z. Chen and H. Luo, *J. Phys. Chem. C*, 2010, **114**, 1901-1911.
5. X. Yuan, Y. Sun and M. Xu, *J. Solid State Chem.*, 2012, **196**, 362-366.
6. S.-Y. Li, G. A. Niklasson and C. G. Granqvist, *J. Appl. Phys.*, 2010, **108**, 063525 (1-8).
7. N. Wang, S. Magdassi, D. Mandler and Y. Long, *Thin Solid Films*, 2013, **534**, 594-598.
8. N. Wang, Y. Huang, S. Magdassi, D. Mandler, H. Liu and Y. Long, *RSC Adv.*, 2013, **3**, 7124-7128.

9. N. R. Mlyuka, G. A. Niklasson and C. G. Granqvist, *Appl. Phys. Lett.*, 2009, **95**, 171909 (1-3).
10. X. Cao, N. Wang, M. Shlomo, M. Daniel and Y. Long, *Science of Advanced Materials*, 2014, **6**, 558-561.
11. J. Zhou, Y. Gao, X. Liu, Z. Chen, L. Dai, C. Cao, H. Luo, M. Kanahira, C. Sun and L. Yan, *Phys Chem Chem Phys*, 2013, **15**, 7505-7511.
12. S. Chen, L. Dai, J. Liu, Y. Gao, X. Liu, Z. Chen, J. Zhou, C. Cao, P. Han, H. Luo and M. Kanahira, *Phys Chem Chem Phys*, 2013, **15**, 17537-17543.
13. P. Jin, G. Xu, M. Tazawa and K. Yoshimura, *Jpn. J. Appl. Phys.*, 2002, **41**, L278-L280.
14. C. Liu, N. Wang and Y. Long, *Appl. Surf. Sci.*, 2013, **283**, 222-226.
15. Z. Chen, Y. Gao, L. Kang, J. Du, Z. Zhang, H. Luo, H. Miao and G. Tan, *Sol Energ Mat Sol C*, 2011, **95**, 2677-2684.
16. X. Cao, N. Wang, J. Y. Law, S. C. J. Loo, S. Magdassi and Y. Long, *Langmuir*, 2014, **30**, 1710-1715.
17. L. Kang, Y. Gao, H. Luo, Z. Chen, J. Du and Z. Zhang, *ACS Applied Materials & Interfaces*, 2011, **3**, 135-138.
18. C. Liu, X. Cao, A. Kamyshny, J. Y. Law, S. Magdassi and Y. Long, *J. Colloid Interface Sci.* (In Press, DOI: <http://dx.doi.org/10.1016/j.jcis.2013.11.028>).
19. Z. Chen, Y. Gao, L. Kang, C. Cao, S. Chen and H. Luo, *J Mater Chem A*, 2014, **2**, 2718-2727.
20. Y. Gao, S. Wang, L. Kang, Z. Chen, J. Du, X. Liu, H. Luo and M. Kanehira, *Energy Environ. Sci.*, 2012, **5**, 8234-8237.
21. G. Tong, Y. Li, F. Wang, Y. Huang, B. Fang, X. Wang, H. Zhu, Q. Liang, M. Yan, Y. Qin, J. Ding, S. Chen, J. Chen, H. Zheng and W. Yuan, *Acta Phys Sin-Ch Ed*, 2013, **62**.
22. P. Kiri, M. E. A. Warwick, I. Ridley and R. Binions, *Thin Solid Films*, 2011, **520**, 1363-1366
23. L. Dai, S. Chen, J. Liu, Y. Gao, J. Zhou, Z. Chen, C. Cao, H. Luo and M. Kanehira, *Phys Chem Chem Phys*, 2013, **15**, 11723-11729.
24. H. G. Schild and D. A. Tirrell, *J Phys Chem-US*, 1990, **94**, 4352-4356.
25. Y. Maeda, T. Nakamura and I. Ikeda, *Macromolecules*, 2002, **35**, 217-222.
26. Y. Uraki, T. Imura, T. Kishimoto and M. Ubukata, *Carbohydr Polym*, 2004, **58**, 123-130.
27. Y. Chen, X. Tang, B. Chen and G. Qiu, *Appl. Surf. Sci.*, 2013, **268**, 332-336.
28. F. Genoveva, S. Kimio, T. Toshiyuki, K. Toshiyuki and Z. Miklós, *J. Mol. Liq.*, 2014, **189**, 63-67.
29. X. Feng, Y. F. Guo, X. Chen, Y. P. Zhao, J. X. Li, X. L. He and L. Chen, *Desalination*, **290**, 89-98
30. H. G. Schild, *Prog. Polym. Sci.*, 1992, **17**, 163-249.
31. Z. Zhang, Y. Gao, Z. Chen, J. Du, C. Cao, L. Kang and H. Luo, *Langmuir*, 2010, **26**, 10738-10744.
32. Y. Zhang, X. Liu, G. Xie, L. Yu, S. Yi, M. Hu and C. Huang, *Materials Science and Engineering: B*, 2010, **175**, 164-171.
33. Y. Ling and M. Lu, *J Polym Res*, 2009, **16**, 29-37.

34. S. J. Kim, H. I. Kim, S. J. Park, I. Y. Kim, S. H. Lee, T. S. Lee and S. I. Kim, *Smart Mater. Struct.*, 2005, **14**, 511-514.
35. J. Du, Y. Gao, H. Luo, Z. Zhang, L. Kang and Z. Chen, *Sol. Energy Mater. Sol. Cells*, 2011, **95**, 1604-1609.
36. T. Takezawa, M. Yamazaki, Y. Mori, T. Yonaha and K. Yoshizato, *J. Cell Sci.*, 1992, **101 ( Pt 3)**, 495-501.
37. H. Lin and Y. Cheng, *Macromolecules*, 2001, **34**, 3710-3715.
38. T. Okano, Y. H. Bae, H. Jacobs and S. W. Kim, *J. Controlled Release*, 1990, **11**, 255-265.
39. D. Schmaljohann, *Adv. Drug Delivery Rev.*, 2006, **58**, 1655-1670.
40. Z. Zhou, S. Zhu and D. Zhang, *J Mater. Chem.*, 2007, **17**, 2428-2433.
41. N. Bertrand, J. G. Fleischer, K. M. Wasan and J. C. Leroux, *Biomaterials*, 2009, **30**, 2598-2605.
42. M. Xiong, B. Gu, J.-D. Zhang, J.-J. Xu, H.-Y. Chen and H. Zhong, *Biosens. Bioelectron.*, 2013, **50**, 229-234.
43. J. Li, X. Gong, X. Yi, P. Sheng and W. Wen, *Smart Mater. Struct.*, 2011, **20**, 075005.
44. I. Idziak, D. Avoce, D. Lessard, D. Gravel and X. Zhu, *Macromolecules*, 1999, **32**, 1260-1263.
45. A. Seeboth, J. Kriwanek, D. Lotzsch and A. Patzak, *Polym. Adv. Technol.*, **13**, 507-512.
46. G. Wyszecki and W. S. Stiles, *Color Science: Concepts and Methods, Quantitative Data and Formulae*, Wiley, New York, 2000.
47. ASTM G173 Standard Tables of Reference Solar Spectral Irradiances: Direct Normal and Hemispherical on a 37° Tilted Surface, Annual Book of ASTM Standards, American Society for Testing and Materials, Philadelphia, PA, USA (2012), Vol. 14.04, <http://rredc.nrel.gov/solar/spectra/am1.5>.
48. B. Stenberg, R. A. Viscarra Rossel, A. M. Mouazen and J. Wetterlind, in *Advances in Agronomy*, ed. L. S. Donald, Academic Press, 2010, vol. **107**, 163-215.
49. C. Ager and N. Milton, *Geophysics*, 1987, **52**, 898-906.
50. P. M. Reddy, M. Taha, P. Venkatesu, A. Kumar and M.-J. Lee, *J. Chem. Phys.*, 2012, **136**, 234904 (1-10).
51. G. Ewing, M. Foster, W. Cantrell and V. Sadtchenko, in *Water in Confining Geometries*, eds. V. Buch and J. P. Devlin, Springer Berlin Heidelberg, 2003, ch. **9**, 179-211.

### List of Figures

Figure 1 Solar light transmitted at temperature lower than  $\tau_c$  (left); Solar light partially blocked at temperature higher than  $\tau_c$  (right)

Figure 2 Temperature dependence of optical transparency of the sample (a) 200  $\mu\text{m}$  thickness PNIPAAm; (c) 52  $\mu\text{m}$  thickness; Trend of optical properties of the sample (b) 200  $\mu\text{m}$  thickness; (d) 52  $\mu\text{m}$  thickness

Figure 3 (a) Optical transmittance spectra of the three samples with different thickness between 20  $^{\circ}\text{C}$  and 40  $^{\circ}\text{C}$ ; (b) Trend of  $\Delta T_{\text{sol}}$ ,  $\Delta T_{\text{lum}}$ ,  $\Delta T_{\text{IR}}$  and  $T_{\text{lum}}$  at 40 $^{\circ}\text{C}$  for different thickness.

Figure 4 Smart hydrogel thin films at room temperature (left) and in sunshine environment at 35  $^{\circ}\text{C}$  (right) with thickness of (a) 26  $\mu\text{m}$ ; (b) 52  $\mu\text{m}$ ; (c) 78  $\mu\text{m}$  and (d) 200  $\mu\text{m}$ .

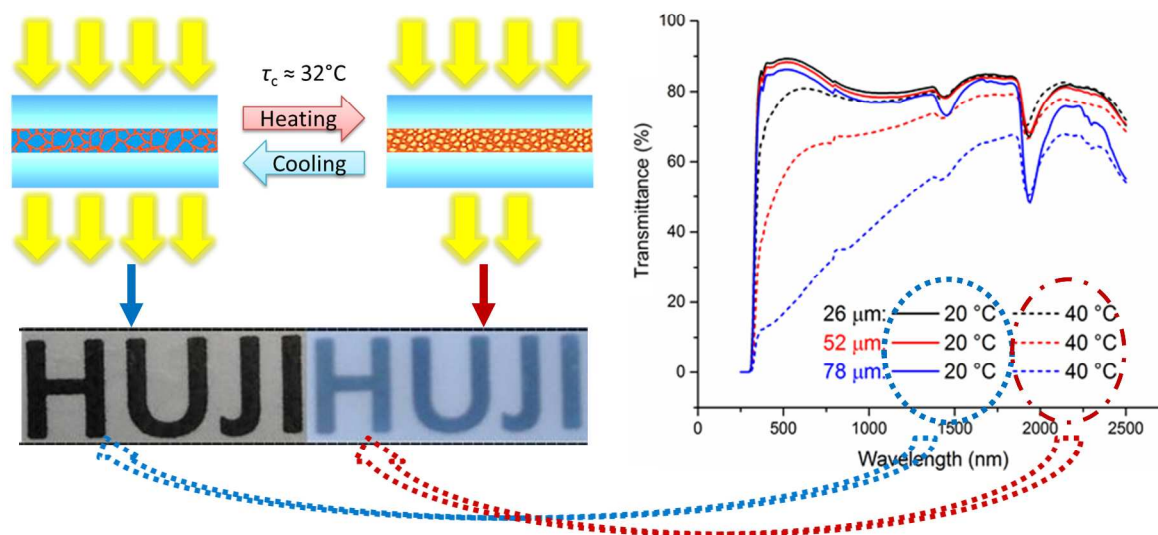
Figure 5 Durability test of hydrogel with thickness of 36  $\mu\text{m}$  between 20  $^{\circ}\text{C}$  and 40  $^{\circ}\text{C}$ .

### List of Tables

Table 1 Thermochromic properties of PNIPAAm hydrogel thin film with 200  $\mu\text{m}$  thickness

Table 2 Thermochromic properties of PNIPAAm hydrogel thin film with 52  $\mu\text{m}$  thickness

Table 1 The optical properties comparison between hydrogel thin film (52  $\mu\text{m}$ ) and  $\text{VO}_2$  thin film



The phase transition of PNIPAm hydrogel at near room temperature make it a potentially good candidate for smart window applications as the high transparency below the transition temperature ( $\tau_c$ ) allows large transmission of solar spectrum radiation while the translucency induced by phase separation above  $\tau_c$  reduces the transmission. With increasing thickness of hydrogel from 26 to 78  $\mu\text{m}$ , the solar modulating ability ( $\Delta T_{\text{sol}}$ ) increases and the luminous transmittance ( $T_{\text{lum}}$ ) decreases. Compared with the best reported results of the most studied inorganic  $\text{VO}_2$  thermochromic coatings, an unprecedented good combination of much higher averaged  $T_{\text{lum}}$  (70.7% v.s 42.8%), higher  $\Delta T_{\text{sol}}$  (25.5% v.s 22.3%) and lower transition temperature ( $\sim 32^\circ\text{C}$  v.s  $\sim 68^\circ\text{C}$ ) could be achieved by hydrogel with 52  $\mu\text{m}$  thickness. The investigation of organic hydrogel in the thermochromic smart windows has been studied for the first time.

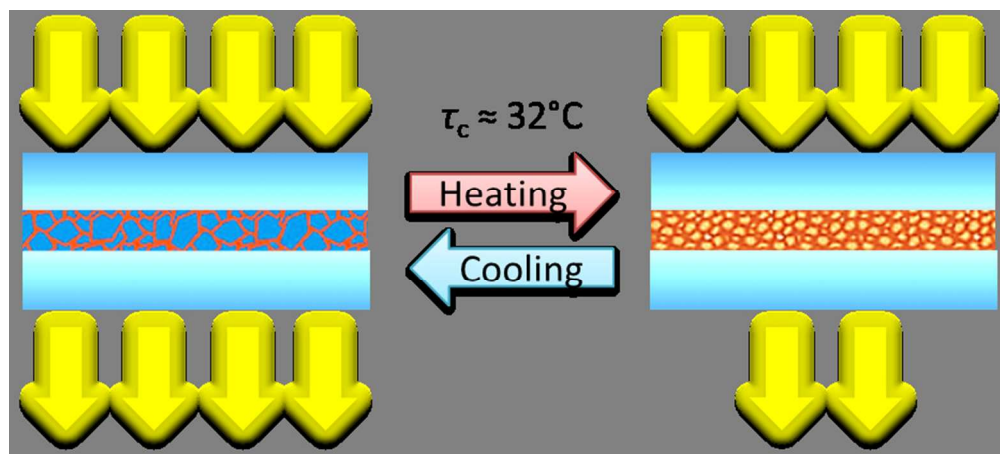


Figure 1 Solar light transmitted at temperature lower than  $\tau_c$  (left); Solar light partially blocked at temperature higher than  $\tau_c$  (right)

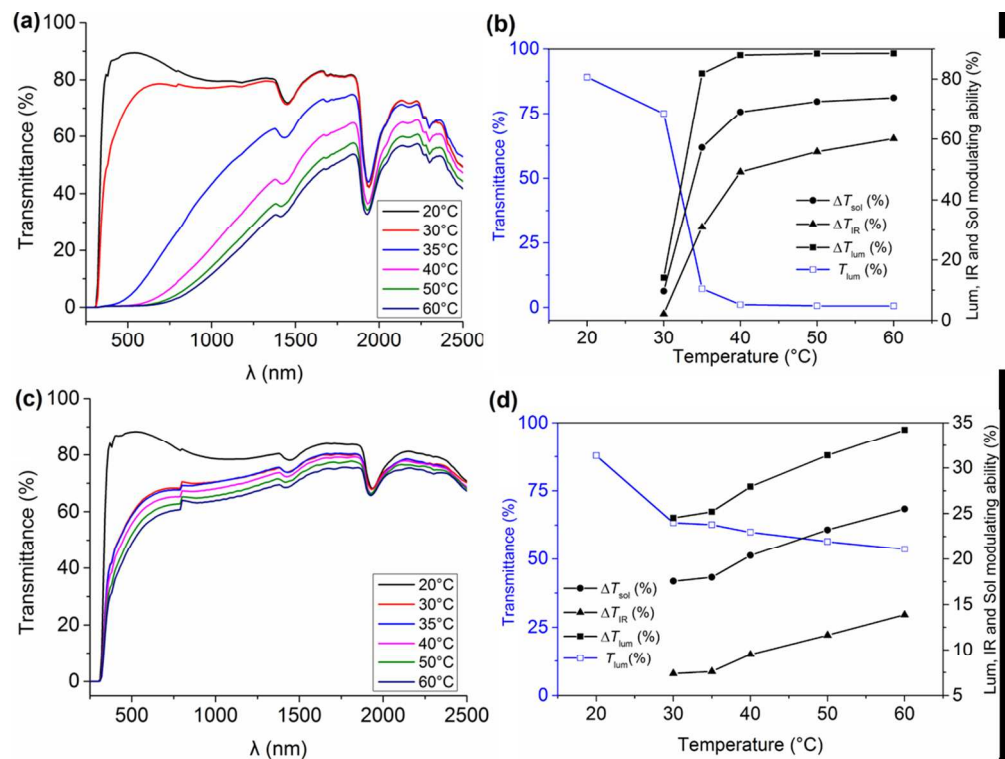


Figure 2 Temperature dependence of optical transparency of the sample (a) 200  $\mu\text{m}$  thickness PNIPAAm; (c) 52  $\mu\text{m}$  thickness; Trend of optical properties of the sample (b) 200  $\mu\text{m}$  thickness; (d) 52  $\mu\text{m}$  thickness

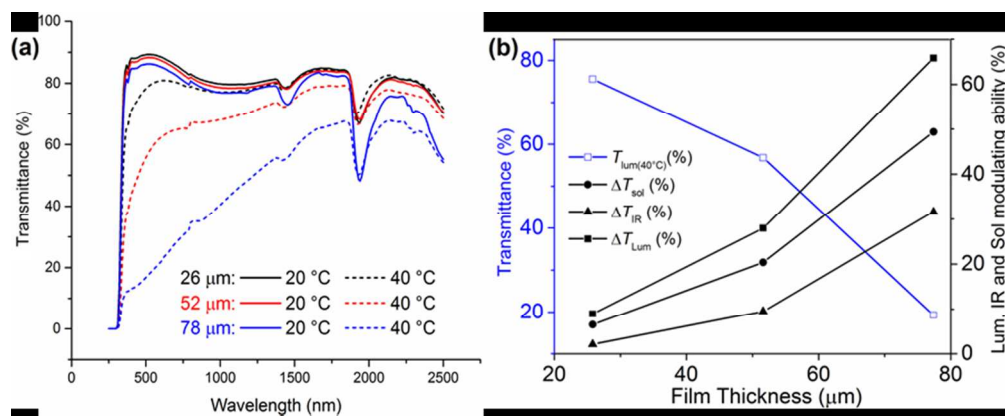


Figure 3 (a) Optical transmittance spectra of the three samples with different thickness between 20 °C and 40 °C; (b) Trend of  $\Delta T_{sol}$ ,  $\Delta T_{lum}$ ,  $\Delta T_{IR}$  and  $T_{lum}$  at 40 °C for different thickness.



Figure 4 Smart hydrogel thin films at room temperature (left) and in sunshine environment at 35 °C (right) with thickness of (a) 26  $\mu\text{m}$ ; (b) 52  $\mu\text{m}$ ; (c) 78  $\mu\text{m}$  and (d) 200  $\mu\text{m}$ .  
107x77mm (120 x 120 DPI)

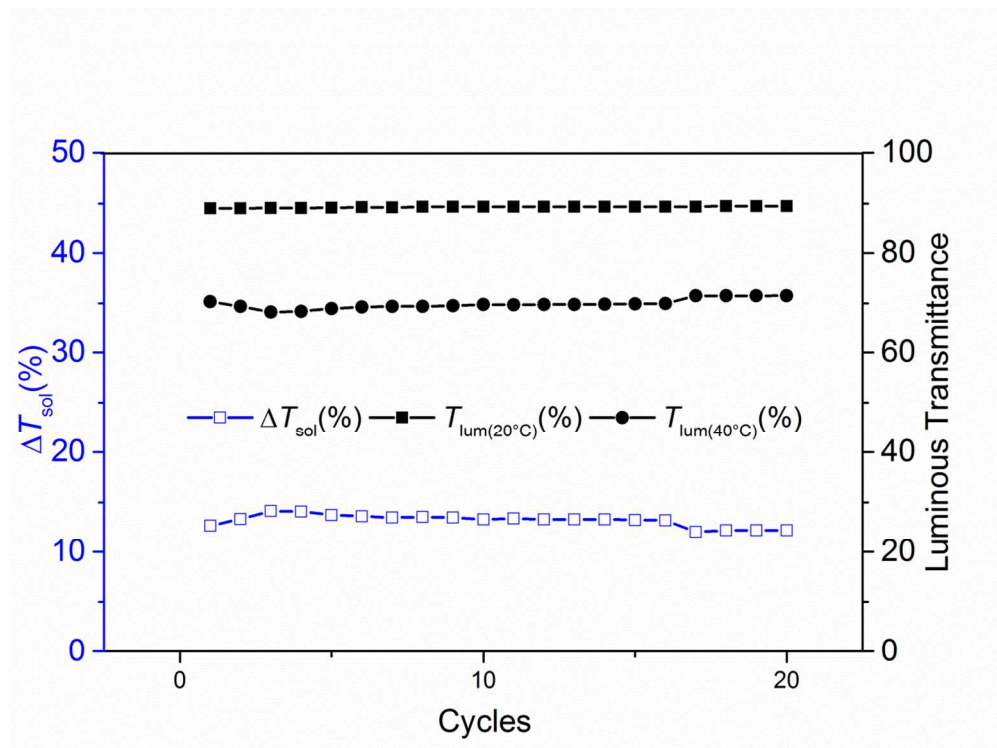


Figure 5 Durability test of hydrogel with thickness of 36  $\mu\text{m}$  between 20  $^{\circ}\text{C}$  and 40  $^{\circ}\text{C}$ .  
349x262mm (96 x 96 DPI)

**Table 1** Thermochromic properties of PNIPAAm hydrogel thin film with 200  $\mu\text{m}$  thickness

200 $\mu\text{m}$	20 °C	30 °C	35 °C	40 °C	50 °C	60 °C
$T_{\text{lum}}$ (%)	89.1	75.0	7.3	1.2	0.7	0.6
$T_{\text{IR}}$ (%)	79.4	77.3	48.4	30.2	23.6	19.3
$T_{\text{sol}}$ (%)	83.3	73.6	57.3	14.2	10.8	9.4

**Table 2** Thermochromic properties of PNIPAAm hydrogel thin film with 52  $\mu\text{m}$  thickness

52 $\mu\text{m}$	20 °C	30 °C	35 °C	40 °C	50 °C	60 °C
$T_{\text{lum}}$ (%)	87.9	63.3	62.6	59.9	56.5	53.6
$T_{\text{IR}}$ (%)	80.0	72.6	72.7	70.5	68.4	66.1
$T_{\text{sol}}$ (%)	83.0	65.5	65.0	62.3	59.8	57.5

Table 3 The optical properties comparison between hydrogel thin film (52  $\mu\text{m}$ ) and  $\text{VO}_2$  thin film

	$T_{\text{lum}(20^\circ\text{C})}$	$T_{\text{lum}(40^\circ\text{C})}$	$\Delta T_{\text{lum}}$	Ave $T_{\text{lum}}$	$T_{\text{sol}(20^\circ\text{C})}$	$T_{\text{sol}(40^\circ\text{C})}$	$\Delta T_{\text{IR}}$	$\Delta T_{\text{sol}}$
<b>26 <math>\mu\text{m}</math></b>	88.9	79.9	9.0	84.4	84.2	77.7 <sup>a</sup>	2.1	6.5
<b>52 <math>\mu\text{m}</math></b>	<b>87.9</b>	<b>59.9</b>	<b>28.0</b>	<b>73.9</b>	<b>83.0</b>	<b>62.7</b>	<b>9.5</b>	<b>20.4</b>
<b>78 <math>\mu\text{m}</math></b>	85.8	19.9	65.9	52.8	81.0	31.6	31.7	49.6
<b><math>\text{VO}_2</math> thin film<sup>16</sup></b>	<b>63.7</b>	$T_{\text{lum}(90^\circ\text{C})}$ <b>54.4</b>	<b>9.3</b>	<b>59.1</b>	<b>61.9</b>	$T_{\text{lum}(90^\circ\text{C})}$ <b>49.9</b>	<b>17.2</b>	<b>12</b>